THE TRANSIENT RESPONSE FOR DIFFERENT TYPES OF ERODABLE SURFACE THERMOCOUPLES USING FINITE ELEMENT ANALYSIS

by

Hussein MOHAMMED, Hanim SALLEH, and Mohd Zamri YUSOFF

Original scientific paper
UDC: 536.532:512.542
BIBLID: 0354-9836, *11* (2007), 4, 49-64

The transient response of erodable surface thermocouples has been numerically assessed by using a two dimensional finite element analysis. Four types of base metal erodable surface thermocouples have been examined in this study, included type-K (alumel-chromel), type-E (chromel-constantan), type-T (copper-constantan), and type-J (iron-constantan) with 50 μm thickness for each. The practical importance of these types of thermocouples is to be used in internal combustion engine studies and aerodynamics experiments. The step heat flux was applied at the surface of the thermocouple model. The heat flux from the measurements of the surface temperature can be commonly identified by assuming that the heat transfer within these devices is one-dimensional. The surface temperature histories at different positions along the thermocouple are presented. The normalized surface temperature histories at the center of the thermocouple for different types at different response time are also depicted. The thermocouple response to different heat flux variations were considered by using a square heat flux with 2 ms width, a sinusoidal surface heat flux variation width 10 ms period and repeated heat flux variation with 2 ms width. The present results demonstrate that the two dimensional transient heat conduction effects have a significant influence on the surface temperature history measurements made with these devices. It was observed that the surface temperature history and the transient response for thermocouple type-E are higher than that for other types due to the thermal properties of this thermocouple. It was concluded that the thermal properties of the surrounding material do have an impact, but the properties of the thermocouple and the insulation materials also make an important contribution to the net response.

Key words: *finite element analysis, transient response, different types erodable surface thermocouples, different heat flux variations*

Introduction

The accurate measurement of heat transfer rates has long been recognized as a key to improvements is such unsteady energy conversion devices as internal combustion engines and aerodynamics vehicles. The heat flow in these devices is usually quite high (hundreds of kilowatts per square meter) and very unsteady. Thus, the requirement, for a

rugged and non-disturbing heat flux sensor with high response, is necessary for these applications. Therefore, the eroding surface thermocouples have been used for many years in various applications including boiling studies [1-6], in the droplets of molten metals [7-11], in internal combustion engine heat flux measurements [12-21], and in aerothermodynamics experiments [22-24] and ballistics research [25]. The eroding surface ribbon element thermocouple is a type of commercially available surface junction thermocouple which has been used in similar applications. The erodable surface thermocouples are often used in internal combustion engine since it is relatively low cost and robust devices with demonstrated delay or rise time typically less than 30 μs [15, 26]. Such fast response times are achieved because a low thermal inertia junction is created by sanding or scratching the surface of the thermocouple by using abrasive paper or scalpel blades, the thermocouple materials themselves form part of the nominally semi-infinite gauge substrate. The eroding thermocouple provides a measurement of temperature close to the surface of the gauge because of low thermal inertia of the junction. In order to identify the instantaneous heat flux from the measured surface temperature history, it is necessary to apply a suitable model for the transient heat conduction process within the surface thermocouple. Most of previous investigators have used the one-dimensional heat conduction model [15, 17, 18, 25]. Under such conditions, the only parameter that enters the analysis for identification of the transient component of the heat flux is the thermocouple thermal product $(\rho ck)^{1/2}$. Many attempts have been made to identify suitable values of $(\rho ck)^{1/2}$ for erodable surface thermocouples through calibration by using the droplet of water and shock tube [26] or using the laser energy pulse applied at the surface of the thermocouple [27], although it sometimes assumed that the thermal properties of the gauge will be dominated by the surrounding material into which the thermocouple is embedded as observed by Oude Nijeweme *et al*. [18]. However, the composite construction of erodable surface thermocouples makes it unlikely that a single value of $(\rho ck)^{1/2}$ can be applied at all frequencies of interest. As discussed by Buttsworth [26] the calibrations to identify $(\rho ck)^{1/2}$ should ideally be performed on the time scales of interest in the actual experiments. However, if the one-dimensional heat conduction assumption is fundamentally flawed for the timescales of interest, even such calibrations may not ensure the accurate deduction of the heat flux.

Therefore, the purpose of this article is to numerically investigate the transient response of two-dimensional finite element (FE) model for four types of erodable surface thermocouples included (type-K, type-E, type-T, and type-J) for different time scales in order to determine the possible limitations of the commonly applied one-dimensional heat conduction assumption also to compare the results of the surface temperature history and the thermal transient response for different thermocouple types.

Theoretical background

The operating principles and typical sensor designs that are employed for transient heat transfer measurements are reviewed by Schultz and Jones [28]. To obtain the fastest possible response from the sensor, it is advantageous to base the heat transfer mea-

surements on temperature data obtained directly at the surface of the body under study. The unsteady conduction of heat within a solid body is described by linear partial differential equations when the temperature gradients remain small. Thus, the heat transfer rates to the surface of a body may be inferred from the time history of temperature measurements made close to the surface by solving the resulting inverse diffusion problem. Common sensing mechanisms for obtaining the required temperature data are the variation of resistivity of a thin metallic film with temperature or the generation of a thermoelectric electromotive force at a junction of dissimilar metals [28]. It is important to recognize that the choice of basic configuration has a significant impact on sensor degradation mechanisms, and thereby the accuracy and robustness of a sensor in hostile flow environments. In order to elucidate the important operating principles and design criteria we briefly review the unsteady, linear conduction of heat in a one-dimensional semi-infinite solid that is described by:

$$\frac{\partial^2 T(x,t)}{\partial x^2} \quad \frac{1}{\alpha}\frac{\partial T(x,t)}{\partial t} \tag{1}$$

where T is the temperature, x is the spatial coordinate normal to the surface, and t is the time. For uniform initial conditionT_i and instantaneously applied, constant surface heat flux q:

$$T(x,t) = T_\mathrm{i} \tag{2}$$

$$\frac{\partial T}{\partial x}_{x\ 0} \quad \frac{q}{k} \tag{3}$$

The solution is known to be:

$$\Delta T \quad T \quad T_\mathrm{i} \quad \frac{2q}{k}\sqrt{\frac{\alpha t}{\pi}}\,\mathrm{e}^{\frac{x^2}{4\alpha t}} \quad \frac{qx}{k}\ 1 \quad \mathrm{erf}\,\frac{x}{2\sqrt{\alpha t}} \tag{4}$$

Approximations to this exact solution are useful because they highlight the key design parameters for practical heat transfer gauges. Expanding this solution asymptotically in powers of t as $t \quad \infty$ at constant x we obtain:

$$\Delta T \quad \frac{2q}{k}\sqrt{\frac{\alpha}{\pi}}\sqrt{t} \quad \frac{q}{k}x \quad \frac{1}{2}\frac{q}{k}\frac{1}{2\sqrt{\alpha t}}x^2\frac{1}{\sqrt{t}} \quad 0\ \frac{1}{\sqrt{t^3}} \tag{5}$$

The first term is asymptotically valid for $x/(\alpha t)^{1/2} < 1$ and expresses the usual result that the surface temperature rises parabolically with time for a constant heat flux. The criterion $x/(\alpha t)^{1/2} < 1$ provides a limit on the required thinness of the surface sensing element for practical designs. The second order term $(q/k)x$ gives the error in the surface temperature measurement associated with this finite thickness and this estimate is valid provided $x/(\alpha t)^{1/4} < 1$.

Consider next the behaviour at small times. Extracting an exponential prefactor and expanding asymptotically as $t \to 0$ at constant x, the leading order behaviour is:

$$\Delta T \quad \frac{4q}{kx^2}\sqrt{\frac{\alpha t}{\pi}}^{3} e^{\frac{x^2}{4\alpha t}} \tag{7}$$

where $-x^2/4\alpha t > 1$.

Erodable surface thermocouples arrangement

The erodable surface thermocouples configuration considered in the present work is shown in fig. 1. It consists of two dissimilar ribbon elements (chromel-alumel for type-K as an example), each 50 μm in thickness, which are insulated from each other and the surrounding material, dural sheets in the present work by mica sheets with a thickness of 5 μm. The same dimensions and the insulation materials have been used for type-E (chromel-constantan), type-T (copper-constantan) and type-J (iron-constantan). The thermocouple surface junctions are created by sanding the surface with very fine abrasive paper or by using scalpel blades. In this process, microscopic elements of thermocouple material bridge the central mica insulation and junctions are made near the surface of the chromel and/or alumel ribbons for type-K (as an example). This is the ribbon element configuration described by Gatowski *et al.* [15], except that the surrounding material is an aluminum alloy as used by Oude Nijeweme *et al*. [18] rather than cast iron. The thermocouple surface junctions will be in contact with fluid flow because the surface junc-

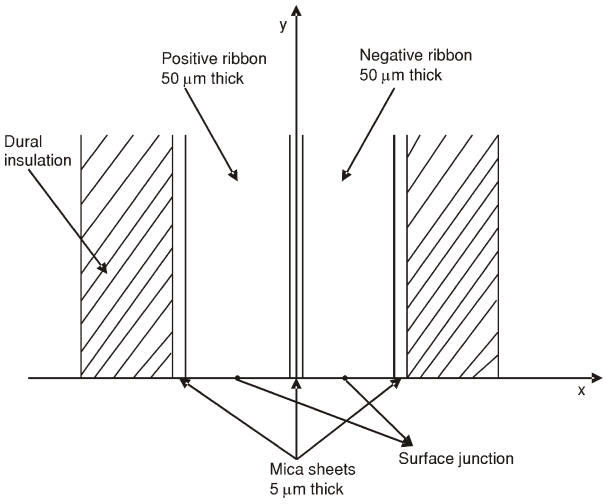

Figure 1. The erodable ribbon element thermocouple geometry

tion of the thermocouple is very close to the surface of measurement and the thermocouple itself placed inside a thread will be flash mounted with the surface of measurement so that contact between the thermocouple sensing junction with the fluid flow will be perfect for a certain environment (like shock tube or internal combustion engines).

Finite element model

For simplification of the FE model, the thermocouple materials for each thermocouple type, K, E, T, and J, were considered as having the same thermal properties (ρ, c, k) (*i. e.* constant properties in x and y directions). Making this assumption, the y-axis in fig. 1 is aligned with a plane of symmetry, and this enables modelling of only half the actual gauge. Although, this assumption is not strictly correct (the actual differences in ρ, c, and k are around 20 percent according to [25, 28], it is reasonable since there are uncertainties in thermal properties (in particular, the thermal conductivity) of mica. Given the above uncertainties and simplifications, round figure estimates for the thermal diffusivity, α, and the thermal product, $(\rho ck)^{1/2}$, of each material and for different thermocouple types were adopted in the analysis as presented in tab. 1.

Table 1. The thermal properties of the mica, dural materials, and the thermocouple types (K, E, T, and J) [25, 28]

Physical properties	Type-K	Type-E	Type-T	Type-J	Dural insulation	Mica sheet
ρ [kgm^{-3}]	8600	8730	8954	7850	2800	2800
c [Jkg^{-1}K^{-1}]	52	448	385	712	1010	56.47
k [Wm^{-1} K^{-1}]	22.36	19.2	39	33.5	141.4	1.581
$(\rho ck)^{1/2}$[Jm^{-2}K^{-1}s$^{-1/2}$]	$10{\cdot}10^{3}$	$8.67{\cdot}10^{3}$	$11.6{\cdot}10^{3}$	$13.7{\cdot}10^{3}$	$20{\cdot}10^{3}$	$0.5{\cdot}10^{3}$
α [m^{2}s^{-1}]	$5{\cdot}10^{-6}$	$4.9{\cdot}10^{-6}$	$1.14{\cdot}10^{-5}$	$6{\cdot}10^{-6}$	$5{\cdot}10^{-5}$	$10{\cdot}10^{-6}$

A FE package, ANSYS 9.0, was used in the current work. Any set of ρ, c, and k values, giving the desired values of α and $(\rho ck)^{1/2}$, could have been chosen for use with the software. Densities close to the physically correct values were chosen for each material and the values of c and k are consistent with the adopted values of α and $(\rho ck)^{1/2}$ were derived (tab. 1). Therefore, we assumed that the thermal properties for each thermocouple are uniform and that the thermocouple materials make perfect thermal contact as previously explained. The heat conduction equations will be solved for the temperature history in a two dimensional model subjected to a uniform surface heat flux by using ANSYS 9.0. The FE model extended to a distance of 0.2 mm in the x-direction and 1 mm in the y-direction. Elements with mid-side nodes were used. At the exposed surface of the thermocouple ($y = 0$), the element length in the y-direction was 0.5 μm. Element lengths

in the y-direction increased with the distance from the surface. At the exposed surface of the thermocouple ($y = 0$), the element length in the x-direction was 0.5 μm within the mica sheets. The surface of the thermocouple material was discretized using elements with an average x length of 1.25 μm with the compression towards the mica material at either edge of the ribbon. The FE equations have been solved by frontal solver program with number of equilibrium iterations of 10000, using the transient integration parameter of 1, with the amplitude decay factor of 0.005, with the oscillation limit criterion of 0.5 and the convergence tolerance of 0.00001. The grit size of the abrasive paper used to create the junctions will affect the thickness of the bridging material, and hence the response of the thermocouple. However, for typical gauge construction, delay or rise times of less than 30 s have been observed by Gatowski *et al*. [15] and Buttsworth [26]. Hence, it was not necessary to model the thermocouple material that bridges the mica insulation, as the timescales of primary interest in the present work are of the order of milliseconds. The accuracy of the FE modelling was assessed by considering a dural sheet with identical dimensions and meshing to the mica sheet running along $\boldsymbol{x} = 0$ boundary in the full mode. A step heat flux of 1 MW/m^2 was applied at the exposed surface of this dural sheet, and the remaining surfaces of the model had zero heat flux boundary conditions. A solution was obtained using a constant time step size of 2.5 μs up to maximum time of 10 ms. Figure 2 shows the surface temperature history produced by the FE modelling normalized using the semi-infinite one-dimensional (si-1D) solution. That is, the surface temperature from FE solution relative to the initial temperature of the material, $T - T_i$, has been divided by the si-1D solution as has been reported by Schultz and Jones [29]:

$$(T \quad T_i)_{\text{si-1D}} \quad \frac{2q\sqrt{t}}{\sqrt{\pi}\sqrt{\rho ck}} \tag{8}$$

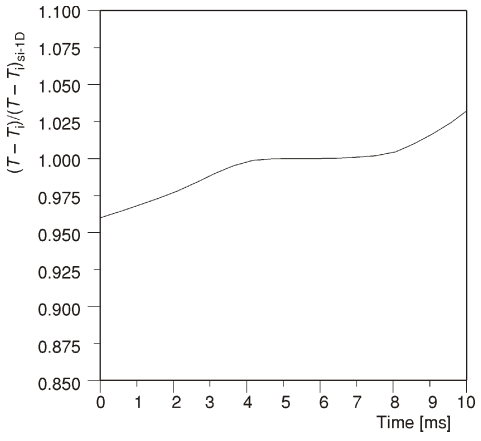

Figure 2. The normalized surface temperature from FE modelling for assessment of accuracy

Following the step in surface heat flux (at $t = 0$), a finite time is required for the FE solution to approach the correct solution, $(T - T_i)/(T - T_i)_{\text{si-1D}} = 1$, as indicated in fig. 2. For the dural material and a time step size of 2.5 μs, approximately 30 μs was required for the surface temperature to approach within 1 percent of the true solution. The FE solution remains within 1 percent of the si-1D solution for up to 7.4 ms. The departure of the FE solution after approximately 7.8 ms (see fig. 2) is due to the zero heat flux boundary condition at $y = 1$ mm (the maximum extent of the model), which results in a more rapid rise in surface temperature than would occur in a si-1D situation.

The erodable surface thermocouple response to a step in surface heat flux

A step heat flux was applied at the surface of the full FE model of the thermocouple. Selected temperature histories from the analysis are presented in figs. 4-7 for type-K, type-E, type-T, and type-J, respectively. It can be seen that the surface tempera-

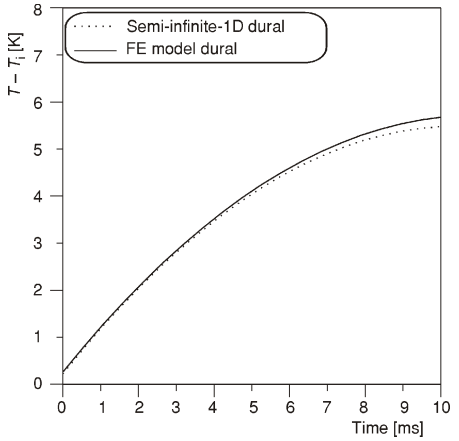

Figure 3. The surface temperature history for dural sheet compared with FE modelling

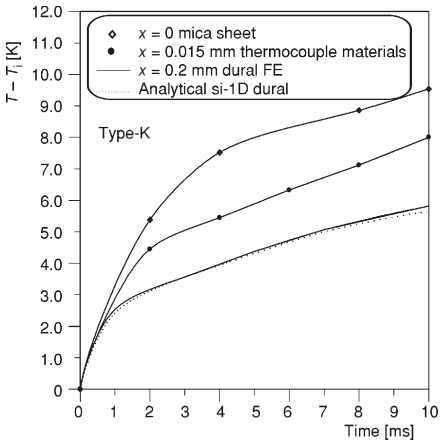

Figure 4. The surface temperature history for different positions along the gauge for type-K

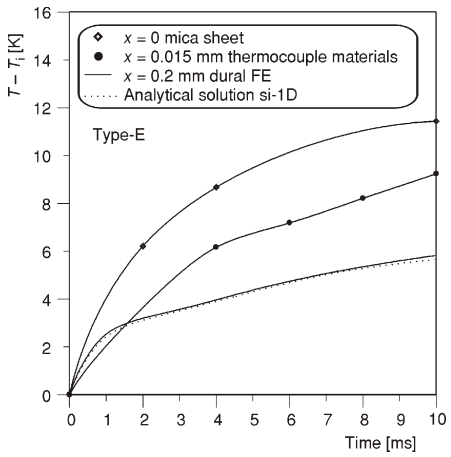

Figure 5. The surface temperature history at different positions along the gauge for type-E

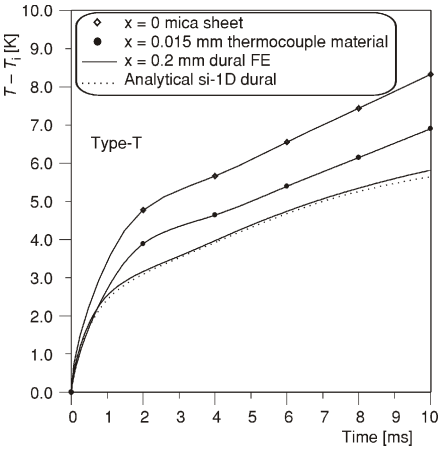

Figure 6. The surface temperature history for different positions along the gauge for type-T

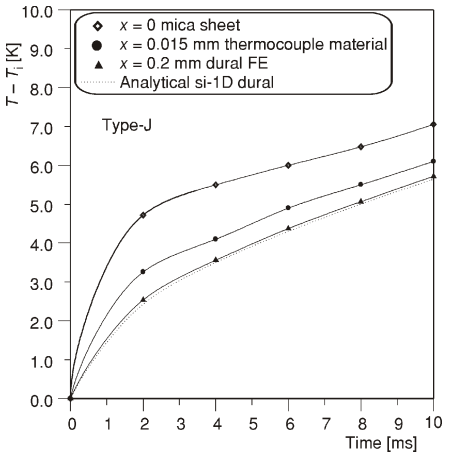

Figure 7. The surface temperature history for different positions along the gauge for type-J

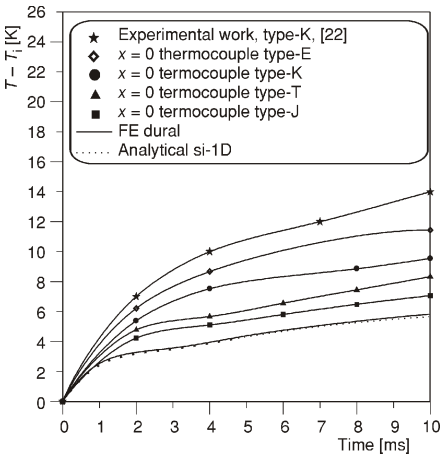

Figure 8. The surface temperature history at $x = 0$ (mica sheet) for different thermocouple types

ture of the mica and thermocouple materials rises faster than that of the dural because of the lower values of $(\rho ck)^{1/2}$ for the mica and thermocouple materials (see tab. 1). The surface temperature of the dural rises faster than the si-1D results (the broken line in fig. 3) because the heat is conducted laterally into the dural from the mica sheet and thermocouple ribbon and the model has a finite extent in the y-direction. The position of the effective junction location on the thermocouple material is probably affected by the abrasive paper grit size used to create the junction, while the junction location will influence the thermocouple response. It was observed that the surface temperature history for thermocouple type-E is higher value than that for other thermocouple types (K, T, and J) due to the thermal properties of this thermocouple ribbon and specifically the thermal conductivity as shown in fig. 8. The thermocouple type-E has excellent thermal and mechanical properties and high thermoelectric power, and it is sometimes used in place of chromel-alumel (type-K) in industrial thermocouples. These types of thermocouples (type-E) have a very fast response time about 100 μs, and are very tough; they can withstand pressures of 600 MPa and temperature fluctuations up to 1600 °C [30]. In addition, the advan-

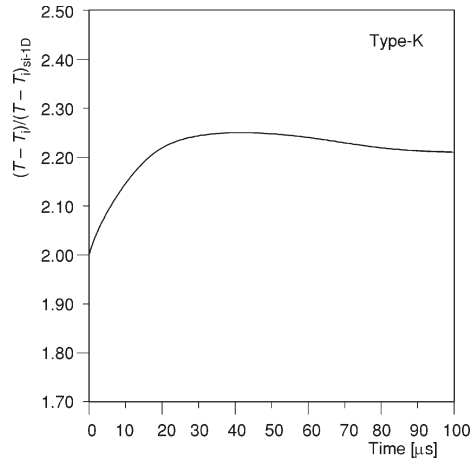

Figure 9. The normalized surface temperature history at the centre of the thermocouple type-K with response to 100 μs

tage of type-E surface thermocouple is has been extensively used for temperature measurements in different experiments as well as different environments. It has moderate sensitivity at low temperatures and a low value of thermal conductivity of the thermocouple materials, makes this thermocouple suitable for low-temperature experiments where small temperature drops are measured. The present results have been compared with the experimental results done by Gai and Joe [22] for type-K. The comparison shows satisfactory agreement and similar trend.

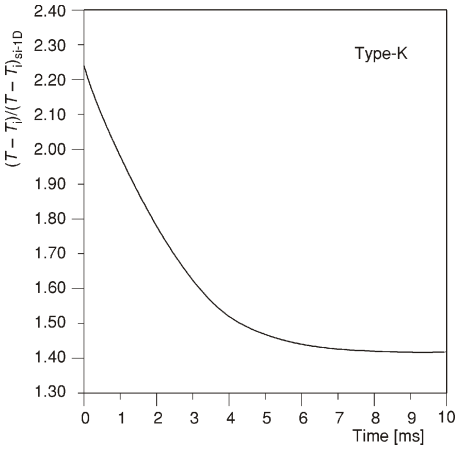

Figure 10. The normalized surface temperature history at the centre of the thermocouple type-K with response to 10 ms

The centre of the ribbon has been chosen as a representative thermocouple junction location. Figure 9 presents the surface temperature history at the centre of the thermocouple ribbon type-K normalized using the si-1D solution with the value of $(\rho ck)^{1/2}$ being that of the dural. For the results presented in fig. 9 for type- K, an initial time step size of 5 ns was taken. This resulted in the finite element solution approaching within 1 percent of the semi-infinite one-dimensional solution $(T - T_i)/(T - T_i)_{si\text{-}1D} = 2$ at $t = 60$ ns. The factor of 2 arises because of the assumed thermal product of the dural material is twice that of the thermocouple material of type-K (tab. 1).

The thermocouple behaves in si-1D manner for only a short time (around 2 μs, see fig. 9) before the surface temperature increases more rapidly owing to the additional heat conduction into the thermocouple ribbon from the mica material. This causes the normalized surface temperature at the thermocouple ribbon surface to rise to a peak value of $(T - T_i)/(T - T_i)_{si\text{-}1D} = 2.24$ at $t = 72$ μs (see fig. 9). After this time, the normalized surface temperature begins to fall owing to lateral conduction of heat away from the thermocouple and mica materials and into the surrounding dural materials. However, fig. 10 indicates that, even at $t = 10$ ms, the thermocouple surface temperature for type-K remains more than 40 percent higher than the an-

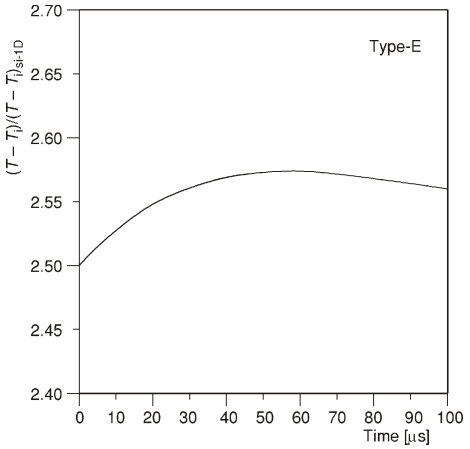

Figure 11. The normalized surface temperature history at the centre of the thermocouple type-E with response to 100 μs

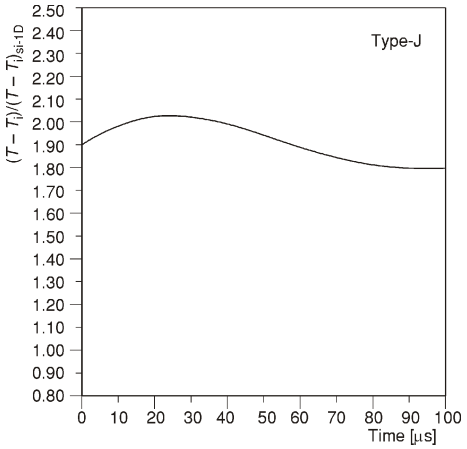

Figure 12. The normalized surface temperature history at the centre of the thermocouple type-J with response to 100 μs

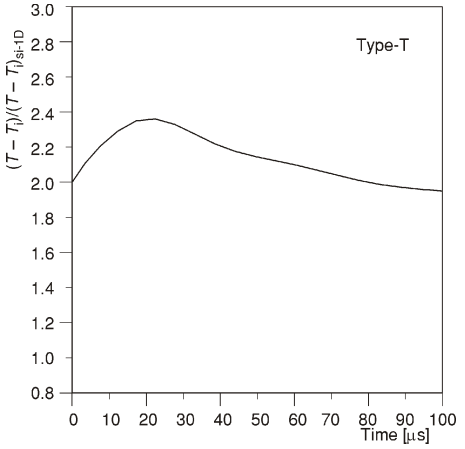

Figure 13. The normalized surface temperature history at the centre of the thermocouple type-T with response to 100 μs

ticipated value for the dural material if si-1D conditions applied. The finite extent of the model in y-direction contributes less than about 5 percent to this difference at t = = 10 ms (see fig. 2).

The normalized surface temperature histories at the centre of the thermocouple ribbon for type-E, type-T, and type-J are presented in figs. 11-13 with response time of 100 μs and which show similar trend and behaviour as mentioned for thermocouple type-K. It was found that the thermocouple type-E has higher response time compared with other thermocouple types as shown in fig. 14 for response time 10 ms. The results presented are qualitatively consistent with the results reported in [25].

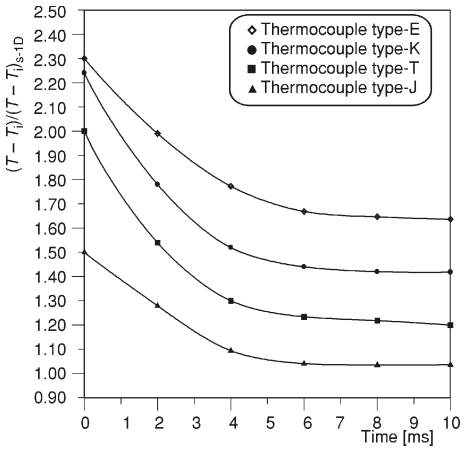

Figure 14. The normalized surface temperature history at the centre of the thermocouple for different types with response to 10 ms

Erodable surface thermocouple response to different heat flux models

To fully specify the problem under consideration, the surface boundary conditions and initial conditions must be provided and these will depend upon the form of the driving surface heat flux to be investigated. Three cases in the present work were consid-

ered: (a) a square heat flux with 2 ms width, (b) a sinusoidal surface heat flux variation width 10 ms period, and (c) repeated heat flux variation with 2 ms width. In the current, the output of the system is the surface temperature at the center of the thermocouple ribbon, and the input to the system is the surface heat flux which is assumed to be uniform across the entire surface of the surface thermocouple. Owing to the linearity of the governing transient heat conduction equations, the heat flux can be considered as a linear system. The system impulse response was identified by differentiating the temperature history obtained from the FE model with a step heat flux input. The thermocouple surface temperature history associated with any particular heat flux history can therefore be simulated through the convolution of the applied heat flux input and the impulse response of the system. To assess the implications of the usual one-dimensional heat conduction assumption, the apparent surface heat flux can be identified from the simulated surface temperature history using:

$$q(t) \quad \frac{\sqrt{\rho ck}}{\sqrt{\pi}} \int_0^t \frac{\mathrm{d}T}{\mathrm{d}\tau} \frac{1}{\sqrt{t \quad \tau}} \mathrm{d}\tau \tag{9}$$

according to Schultz and Jones [29], and compared with the actual heat flux input at the surface of the gauge. The value of $(\rho ck)^{1/2}$ used in eq. (9) was that of the dural material (tab. 1).

The analysis described above has been done for three models of surface heat flux histories. The first model history is a square heat flux pulse of 2 ms width – actual (a) in fig. 15, the second is a sinusoidal heat flux variation with a period of 10 ms – actual (b) in fig. 15, and the third is a repeated step heat flux variation with 2 ms width – actual (c) in fig. 15. For the square heat flux pulse, the apparent heat flux initially exceeds the actual heat flux by more than a factor of 2 because the initial transient conduction process is dominated by the thermocouple and mica materials, rather than by the surrounding dural material. The lateral conduction effects are responsible for the observed form of the apparent heat flux which have already been discussed in the previous section. An important consequence of the lateral conduction is the negative overshoot that occurs at the trailing edge of the pulse. In the present case the apparent heat flux drops to around –0.7 MW/m^2, or about –30 percent of the apparent peak value.

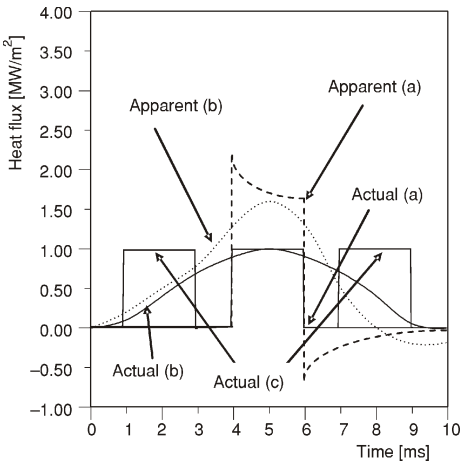

Figure 15. Errors ilustration introduced by one-dimensional treatment
(a) square heat flux pusle of 2 ms width, (b) sinusoidal heat flux variation with a 10 ms period, (c) repeated heat flux variation with 2 ms width

The aim of using the sinusoidal variation in actual heat flux – actual (b) in fig.

15, and the repeated step heat flux variation – actual (c) in fig. 15, was to provide a variation somewhat representative of the heat flux pulses observed in internal combustion engines experiments. The apparent heat flux still deviates substantially from the actual heat flux for the sinusoidal case. The peak heat flux is more than 50 percent higher than the actual heat flux because the thermal properties of the embedded ribbon and mica differ from those of the surrounding dural material. A negative overshoot in the heat flux also occurs for the sinusoidal variation, although it is less significant than for the square pulse. It was observed that for the third repeated heat flux model, the apparent heat flux initially exceeds the actual heat flux by more than a factor of 2 because the domination of the thermocouple and mica materials, rather than the surrounding dural material on the initial transient conduction process and also due to the lateral conduction effects. The negative overshoot that occurs at the trailing edge of the repeated heat flux was also observed and it's around –30 percent of the apparent peak value. Because of the limited space of the paper length, the apparent of case (c) was not shown since it shows the same trend as mentioned for the square heat flux pulse. However, by 10 ms the finite extent of the finite element model in the y-direction influences the results, and tending to reduce the magnitude of the apparent heat flux overshoot relative to the value that would be obtained with a more extensive finite element model.

Error sources

The observed error sources in this analysis include gauge design, material property variations, and lateral conduction heat transfer and the gauge geometry (*i. e.*, the gauge symmetry). We assert that this residual variance, along with variance in the predicted heat flux, reconciles any discrepancies observed in the heat flux results (see fig. 15) relative to the established predictions by analytical solutions. Further errors are associated with the uncertainty in the physical properties of the thermocouple materials, the difference in α and k for the two dissimilar metal conductors and the reduced heat conduction away from the surface may this will be eliminated by experimental calibration. Under these conditions more extreme than those reported here, the physical properties of the thermocouple materials change significantly with temperature. The remaining systematic error due to the finite thickness of the surface junction so that the experimental calibration allows reduction of these error sources to any desired level of accuracy.

Conclusions

Four types of erodable surface thermocouples ribbon element configurations have been considered and numerically assessed in this study. The purpose of this work is to provide applicable results to commonly used thermocouple types and also another intention is to alert the workers to possible errors arising from the accepted one-dimensional modelling of similar erodable thermocouple construction. There are certain limitations of the present work including the non-semi-infinite boundary conditions and

material property uncertainties (particularly for the insulating material). For the timescales of interest in internal combustion engine experiments, it is incorrect to assume that the response of the gauge is governed by the thermal properties of the surrounding material. The thermal properties of the surrounding material do have an impact, but the properties of the thermocouple and the insulation materials also make an important contribution to the net response.

A one-dimensional treatment of the transient surface temperature data produced using these types of erodable surface thermocouples appear inappropriate for the timescales of interest in internal combustion engine experiments. Significant lateral conduction occurs for events with timescales of between 1 and 10 ms (or more). This lateral conduction can result in an apparent (negative) overshoot in response when the level of heating is reduced (if the analysis assumes one-dimensional behaviour). Such a situation arises during the expansion stroke of an internal combustion engine, and negative heat flux values have been registered for both motored engine by Lawton [17] and fired engine by Oude Nijeweme *et al*. [18] even when the gas temperature remains higher than the surface temperature. The negative heat flux results have previously been explained using unsteady boundary layer models by Oude Nijeweme *at al.* [18] and Piccini *et al.* [19]. However, the present results suggest that some portion of the negative heat flux may actually be an artifact from the one-dimensional transient heat conduction modelling.

It was observed from this analysis that the surface temperature of the mica and thermocouple materials rises faster than that of the dural because of the lower values of $(\rho ck)^{1/2}$ for the mica and thermocouple materials. The surface temperature of the dural rises faster than the semi-infinite one-dimensional result because of the heat is conducted laterally into the dural from the mica sheet and thermocouple ribbon. It was also found that the thermocouple type-E has higher response time compared with other thermocouple types (K, T, and J). Finally, if erodable surface thermocouples are to be used for transient heat flux measurements, the transient response of the gauge should be confirmed for the timescales of interest using finite element analysis along the lines described in this work and/or a suitable calibration technique given by Gatowski *et al*. [15] and Buttsworth [26]. If the transient conduction within the thermocouple can not be treated in a one-dimensional manner, a two-dimensional analysis may be possible with the aid of FE modelling to analyze such erodable thermocouples. The experimental work for the fabrication of four types of these surface thermocouples are on going in order to validate the numerical thermal transient response under step heat flux boundary condition. The present results have been compared with the experimental results given by Gai and Joe [22] as shown in fig. 8 and it shows satisfactory agreement and similar trend.

Nomenclature

c – specific heat, [$Jkg^{-1}K^{-1}$]
k – thermal conductivity, [$Wm^{-1}K^{-1}$]
q – surface heat flux, [Wm^{-2}]
t – time, arbitrary or relative to the start of heating [s]

T – temperature at the surface of the gauge, [K]
T_i – initial temperature of the gauge, [K]
x – lateral distance from the center of the gauge, [m]
y – distance (depth) from the surface of the gauge, [m]

Greek letters

α – thermal diffusivity (= $k/\rho c$), [m^2s^{-1}]
ρ – density, [kgm^{-3}]
τ – dummy variable for integration with respect to time, [s]

Subscript

si-1D – semi-infinite one-dimensional

Acknowledgments

The authors wish to highly acknowledge the Ministry of Science Technology and Innovation (MOSTI) and the University Tenaga Nasional for supporting this work under IRPA project with code no. 03-99-03-10002-EAR. Ms. Roslah Johari (UNITEN-library) is also thanked for her diligent and magnificent efforts.

References

[1] Chen, J. C., Hsu, K. K., Heat Transfer during Liquid Contact on Superheated Surfaces, *Journal of Heat Transfer, ASME Trans.*, *117* (1995), 8, pp.693-697
[2] Lee, L., Chen, J. C., Nelson, R. A., Surface Probe for Measurement of Liquid Contact in Film Transition Boiling on High Temperature Surfaces, *The Review of Scientific Instruments*, *53* (1982), 9, pp. 1472-1476
[3] Lee, L. Y. W., Chen, J. C., Nelson, R. A., Liquid-Solid Contact Measurements Using a Surface Thermocouple Temperature Probe in Atmospheric Pool Boiling Water, *Journal of Heat Mass Transfer, 28* (1985), 8, pp.1415- 1423
[4] Bendersky, D., A Special Thermocouple for Measuring Transient Temperatures, *Mech. Eng., 75* (1953), 2, pp. 117-121
[5] Kovas, A., Mesler, R. B., Making and Testing Small Surface Thermocouples for Fast Response, *The Review of Scientific Instruments, 35* (1964), 4, pp. 485-488
[6] Ongkiehong, L., Van Duijn, J., Construction of a Thermocouple for Measuring Surface Temperatures, *J. Scientific Instrum., 37* (1960), 4, pp. 221-222
[7] Moore, F. D., Mesler, R. B., The Measurements of Rapid Surface Temperature Fluctuations during Nucleate Boiling of Water, *AICHE Journal, 7* (1961), 12, pp. 620-624
[8] Guo, S. M., Spencer, M. C., Lock, G. D., Jones, T. V., Harvey, N. W., The Application of Thin Film Gauges on Flexible Plastic Substrates to the Gas Turbine Situation, *ASME 95*-GT-357, 1995
[9] Heichal, Y., Chandra, S., Bordatchev, E., A Fast-Response Thin Film Thermocouple to Measure Rapid Surface Temperature Changes, *Experimental Thermal and Fluid Science*, *30* (2005), 2, pp. 153-159

[10] Tong, H. M., Arjavalingam, G., Haynes, R. D., Hyer, G. N., Ritsko, J. J., High-Temperature Thin-Film Pt-Ir Thermocouple with Fast Response Time, *The Review of Scientific Instruments*, *58* (1987), 5, pp. 875-877
[11] Epstien, A. H., Guenette, G. R., Norton, R. J., Yuzhang, C., High Frequency-Response Heat Flux Gauge, *The Review of Scientific Instruments, 57* (1986), 4, pp. 639-649
[12] Alkidas, A. C., Myers, J. P., Transient Heat Flux Measurements in the Combustion Chamber of a Spark Ignition Engine, *Journal of Heat Transfer, ASME Trans.*, *104* (1982), 2, pp. 62-67
[13] Alkidas, A. C., Heat Transfer Characteristics of a Spark Ignition Engine, *Journal of Heat Transfer ASME Trans.*, *102* (1980), 5, pp. 189-193
[14] Alkidas, A. C., Cole, R. M., Transient Heat Flux Measurements in a Divided Chamber Diesel Engine, *Journal of Heat Transfer, ASME Trans.*, *107* (1985), 5, pp. 439-444
[15] Gatowski, J. A., Smith, M. K., Alkidas, A. C., An Experimental Investigation of Surface Thermometry and Heat Flux, *Experimental Thermal and Fluid Science, 2* (1989), 3, pp. 280-292
[16] Wilson, T. S., Bryanston-Cross, P., Chana, K. S., Dunkley, P., Jones, T. V., Hannah, P., High Bandwidth Heat Transfer and Optical Measurements in an Instrument Spark Ignition Internal Combustion Engine, *SAE paper* 2002-01-0747, 2002
[17] Lawton, B., Effect of Compression and Expansion on Instantaneous Heat Transfer in Reciprocating Internal Combustion Engines, *Proc. Instn. Mech. Engrs., Part A, Journal of Power and Energy*, *201* (1987), A3, pp. 175-186
[18] Oude Nijeweme, D. J., Kok, J. B. W., Stone, C. R., Wyszynski, L., Unsteady in-Cylinder Heat Transfer in a Spark Ignition Engine: Experiments and Modelling, *Proc. Instn Mech. Engrs., Part D, Journal of Automobile Engineering, 215* (2001), Part D, pp. 747-760
[19] Piccini, E., Guo, S. M., Jones, T. V., The Development of a New Direct-Heat Flux Gauge for Heat Transfer Facilities, *Measmt. Sci. Technol., 11* (2000), 3, pp. 342-349
[20] Rakopoulos, C. D., Mavropoulos, G. C., Experimental Instantaneous Heat Fluxes in the Cylinder Head and Exhaust Manifold of an Air-Cooled Diesel Engine, *Energy Convers. Mgmt., 41* (2000), 12, pp. 1265-1281
[21] Yamada, Y., Emi, M., Ishii, H., Suzuki, Y., Kimura, S., Enomoto, Y., Heat Loss to the Combustion Chamber Wall with Deposit in D. I. Diesel Engine: Variation of Instantaneous Heat Flux on Piston Surface with Deposit, *JSAE Review, 23* (2002), 4, pp. 415-421
[22] Gai, S. L., Joe, W. S., Laminar Heat Transfer to Blunt Cones in High-Enthalpy Flows, *J. Thermophysics Heat Transfer, 6* (1992), 3, pp. 433-438
[23] Lees, L., Laminar Heat Transfer over Blunt Nosed Bodies at Hypersonic Flight Speeds, *Journal of Jet propulsions*, *26* (1956), 2, pp. 259-268
[24] Jessen, C., Vetter, M., Gronig, H., Experimental Studies in the Aachen Hypersonic Shock Tunnel, *Z. Flugwiss. Weltraumforsch*, *17* (1993), 1, pp. 73-81
[25] Lawton, B., Klingenberg, G., Transient Temperature in Engineering and Science, Oxford University Press, Oxford, UK, 1996
[26] Buttsworth, D. R., Assessment of Effective Thermal Product of Surface Junction Thermo-Couples on Millisecond and Microsecond Time Scales, *Experimental Thermal and Fluid Science, 25* (2001), 6, pp. 409-420
[27] Lyons, P. R. A., Gai, S. L., A Method for the Accurate Determination of the Thermal Product for Thin Film Heat Transfer or Surface Thermocouple Gauges, *J. Phys. E: Sci Instrum*, *21* (1988), 6, pp. 445-448
[28] Caldwell, F. R., Thermocouple Materials, in: Temperature Measurement and Control in Science and Industry (Ed. C. M. Herzfeld), *Applied Methods and Instruments, 3* (1962), pp. 81-134
[29] Schultz, D. L., Jones, T. V., Heat-Transfer Measurements in Short-Duration Hypersonic Facilities, AGARDOgraph 165, Advisory Group for Aerospace Research and Development, Brussels, 1973
[30] Dike, P. H., Thermoelectric Thermometry, Leeds and Northrup Company, Philadelphia, Penn., USA, 1954, pp. 15

Author's address:

H. Mohammed, H. Salleh, M. Z. Yusoff
University Tenaga Nasional, College of Engineering,
Mechanical Engineering Depatrment,
Km7, Jalan Kajang – Puchong, 43009 Kajang,
Selangor, Malaysia

Corresponding author H. A. Mohammed
E-mail: hussein@uniten.edu.my

Paper submitted: December 1, 2006
Paper revised: July 11, 2007
Paper accepted: October 10, 2007